Journal of Neuroimmunology 332 (2019) 198–211

Contents lists available at ScienceDirect

Journal of Neuroimmunology

journal homepage: www.elsevier.com/locate/jneuroim

Long-term actions of interleukin-1β on K^+, Na^+ and Ca^{2+} channel currents in small, IB_4-positive dorsal root ganglion neurons; possible relevance to the etiology of neuropathic pain

Myung-chul Noh[a], Patrick L. Stemkowski[b,1], Peter A. Smith[a,b,*]

[a] Department of Pharmacology, University of Alberta, Edmonton, Alberta T6G 2H7, Canada
[b] Neuroscience and Mental Health Institute, University of Alberta, Edmonton, Alberta T6G 2H7, Canada

ARTICLE INFO

Keywords:
Nerve injury
Ion channel
Neuroinflammation
Primary afferent
Peripheral neuropathy
K^+ channel
Na^+ channel
BK(Ca) channel
Nociceptor
Electrophysiology

ABSTRACT

Excitation of dorsal root ganglion (DRG) neurons by interleukin 1β (IL-1β) is implicated in the onset of neuropathic pain. To understand its mechanism of action, isolectin B4 positive (IB_4^+) DRG neurons were exposed to 100pM IL-1β for 5-6d. A reversible increase in action potential (AP) amplitude reflected increased TTX-sensitive sodium current (TTX-S I_{Na}). An irreversible increase in AP duration reflected decreased Ca^{2+}- sensitive K^+ conductance (BK(Ca) channels). Different processes thus underlie regulation of the two channel types. Since changes in AP shape facilitated Ca^{2+} influx, this explains how IL-1β facilitates synaptic transmission in the dorsal horn; thereby provoking pain.

1. Introduction

A common approach to the study of neuropathic pain involves analysis of the response of the somatosensory system to peripheral nerve injury (Decosterd and Woolf, 2000; Kim et al., 1997; Stemkowski and Smith, 2013; Sandkuhler, 2009; Alles and Smith, 2018). Following injury, a transient inflammatory response leads to increased excitability of primary afferent neurons (Grace et al., 2014; Scholz and Woolf, 2007; Watkins and Maier, 2002; Basbaum et al., 2009) and the generation of spontaneous, ectopic activity (Vaso et al., 2014; Wall and Devor, 1983; Abdulla and Smith, 2001a; Koplovitch and Devor, 2018; Djouhri et al., 2006). This, in turn, elicits enduring changes in synaptic transmission in the spinal superficial laminae (Sandkuhler, 2009; Coull et al., 2003; Balasubramanyan et al., 2006; Chen et al., 2016; Alles and Smith, 2018) and an overall increase in dorsal horn excitability known as central sensitization (Woolf, 1983; Basbaum et al., 2009; Grace et al., 2014).

Nerve injury increases the level of the pro-inflammatory cytokine, interleukin 1β (IL-1β) in sciatic nerve and DRG (Nadeau et al., 2011). Systemic administration IL-1β is also known to generate hyperalgesia (Ferreira et al., 1988). This, and the observation that antibodies to interleukin 1-receptor (IL-1R) or its genetic deletion or overexpression of interleukin receptor antagonist reduce pain behavior in mice with experimental neuropathy has led to IL-1β being implicated in the onset of neuropathic pain (Sommer et al., 1999; Sommer and Kress, 2004; Scholz and Woolf, 2007; Moalem and Tracey, 2006; Wolf et al., 2006). Further support for this idea comes from the observation that the excitability of the cell bodies of sensory neurons in the dorsal root ganglion (DRG) is increased following acute (Binshtok et al., 2008) or long-term exposure to IL-1β (Stemkowski and Smith, 2012a; Stemkowski et al., 2015; Stemkowski and Smith, 2012b). By inducing long-term changes in the excitability of sensory nerves, it indirectly drives increased excitability in the spinal dorsal horn and the development (Vaso et al., 2014) and persistence of central sensitization (Pitcher and Henry, 2008).

The level of bioactive IL-1β in peripheral nerve reaches a peak at 7d after injury (Nadeau et al., 2011). We have therefore studied its long-term actions and found that exposure to IL-1β (100 pM) for 5-6d produces different effects in different types of DRG neuron. Medium-sized DRG neurons, which are the cell bodies of Aδ-fibres (Harper and Lawson, 1985) and which usually carry nociceptive information, were the most profoundly affected. Excitability was increased and action

* Corresponding author at: Department of Pharmacology, 9-75 Medical Sciences Building, University of Alberta, Edmonton, AB T6G 2H7, Canada.
E-mail address: pas3@ualberta.ca (P.A. Smith).
[1] PLS present address: Inscopix Inc., 2462 Embarcadero Way, Palo Alto, CA, 94303, USA.

https://doi.org/10.1016/j.jneuroim.2019.05.002
Received 19 February 2019; Received in revised form 18 April 2019; Accepted 1 May 2019
0165-5728/

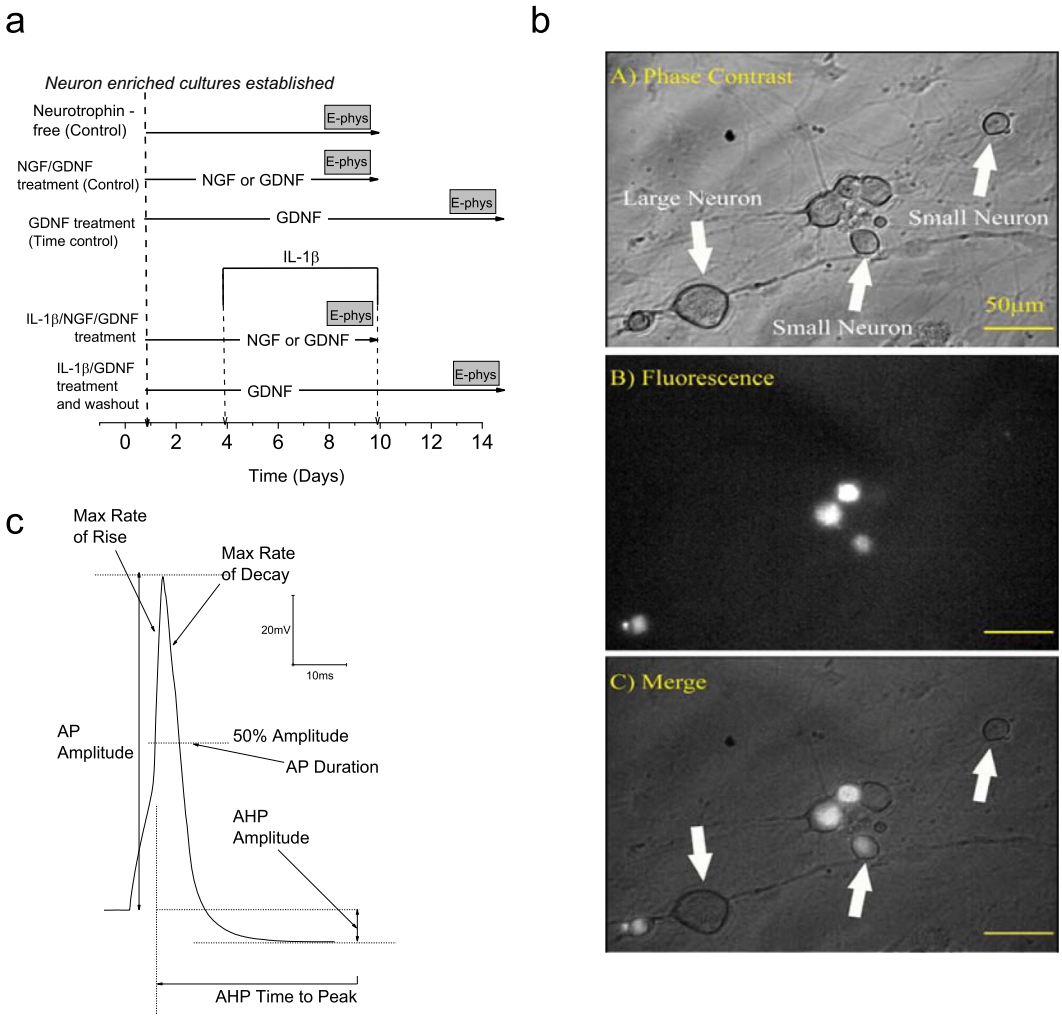

Fig. 1. a. Scheme to show time course of exposure to IL-1β, NGF or GDNF from time of establishment of neuron enriched cultures. Grey bars indicate during periods in which electrophysiological recordings were made. **b.** Photomicrographs to illustrate IB_4^+ and IB_4^- neurons identified by IB_4 Alexa Fluor 488 congugate. Phase contrast and fluorcence images are displayed and superimposed. **c.** Action potential (AP) parameters mesured in small IB_4^+ neurons.

potential afterhyperpolarization was attenuated as a result of a reversible decrease in voltage sensitive K^+ currents. Thus, the amplitudes of A-current, delayed rectifier and Ca^{2+}-sensitive K^+ currents were reduced by 68%, 64% and 36%, respectively with only modest effects on Na^+ and Ca^{2+} channel currents (Stemkowski et al., 2015). Since the properties and amplitudes of K^+ channel currents recorded in neurons 3-4d after expose to cytokine for 5-6d were no different from those seen in time matched controls, the actions of IL-1β appeared to be reversible. This cytokine does not appear to initiate an enduring shift in the electrophysiological phenotype of medium-sized DRG neurons.

Large neurons (presumed cell bodies of Aβ fibres) and those small C-fibre nociceptors which fail to bind the *Griffonia simplicifolia* lectin, IB_4 were little affected by IL-1β. By contrast, the action potential (AP) duration of small IB_4-positive neurons was increased by 35% and this was mediated by IL-1R and accompanied by a slight increase in excitability (Stemkowski and Smith, 2012a; Stemkowski et al., 2015). Here we investigate the changes in ion channel properties that underlie the effects of IL-1β as several lines of evidence implicate small, $IB4^+$ neurons in both the etiology of various types of neuropathic pain (Taylor et al., 2012; Li and Zhou, 2001; Bogen et al., 2009; Yilmaz et al., 2017; Bautzova et al., 2018) and in hyperalgesic priming (Ferrari et al., 2010)

2. Materials and methods

2.1. Ethical approval

All procedures were reviewed and approved by the University of Alberta Health Sciences Laboratory Animal Services Welfare Committee, which is responsible for compliance with the guidelines of the Canadian Council for Animal Care.

2.2. Primary neuronal cultures

Neuron enriched, defined medium cultures were prepared as described previously using p16–20 male Sprague-Dawley rats which were euthanized with an IP injection of 1.5 g/kg urethane (Stemkowski et al., 2015; Stemkowski and Smith, 2012a). Thoracic and lumbar DRGs were collected in Dulbecco's modified Eagle's medium (DMEM) supplemented with 10% heat-inactivated horse serum (DMEMHS; both from Gibco, Grand Island, NY, USA). Tubes containing ganglia were shaken at 1 Hz for 1.5 h at 34 °C with DMEMHS containing 0.125% type IV collagenase (Worthington, Lakewood, NJ, USA), washed twice in Ca^{2+}-free phosphate buffered saline (PBS), treated with 0.25% trypsin from bovine pancreas (Sigma) in PBS for 30 min, washed 3 times in DMEMHS and finally taken up in 2 ml of DMEMHS containing 80 μg/ml type IV DNAse (Sigma) and 100 μg/ml soybean trypsin inhibitor (Worthington

Biochemical Corporation, Lakewood, NJ, USA). A suspension of single cells was obtained by trituration of the enzymatically softened ganglia by 6–8 passages through the tip of a 1 ml Eppendorf pipette.

To minimize the proliferation of non-neuronal cells, dissociated ganglia were pre-plated in DMEMHS that was supplemented with cytosine 3-D-arabino-furanoside (Ara−C), uridine and 5-fluoro-2′-deoxyuridine (all from Sigma and all at 10 μM) in culture dishes (Corning, NY, USA) previously coated with 3 μg/ml polyornithine (Sigma). After 15–20 h, the non-neuronal cells become firmly attached to the dish, while most of the neurons were only weakly adherent. Most dead cells and axonal/myelin debris were discarded by removing the culture medium prior to selectively dislodging the attached neurons with a gentle stream of serum-free defined medium (F12, DMEM supplemented with 1/100 N-2 supplement and 1/100 Penicillin/Streptomycin/Amphotericin B (all from Gibco). Neurons from the two preplates were collected in 12 ml of serum free defined medium. Further neuronal enrichment was achieved by centrifugation of the cell suspension at 500 rpm for 5 min, whereupon viable neurons are lightly pelleted, leaving myelin debris, dead cells and small non-neuronal cells in suspension. The supernatant was discarded and the pelleted cells re-suspended in 1 ml of serum free defined medium. At 100 μl volumes, the cells were plated into 35 mm tissue culture dishes (Nunc, Roskilde, Denmark) pre-coated with 3 μg/ml polyornithine (Sigma) and 2 μg/ml laminin (Sigma). All dishes were then filled with a neurotrophin- and serum-free defined medium at ~ 2 ml/dish. Cells were maintained at 36.5 °0C, 95% air, 5% CO_2. Defined medium was exchanged every 72 h. Cultures were exposed to 100 pM IL-1β (Peprotech, Rocky Hill, NJ, USA; prepared in 0.1% BSA (Sigma)) for 5 – 6d as per our previous studies (Stemkowski and Smith, 2012a; Stemkowski et al., 2015). Neurons in time matched cultures treated with 0.1% BSA alone with or without GDNF or NGF served as controls (Fig. 1a). For washout of IL-1β, medium was exchanged every 72 h for 3–4 days. Medium was exchanged three times at each time point to facilitate cytokine removal. This washing procedure was deemed appropriate as it allowed for partial recovery of IL-1β effects in our previous study of medium sized DRG neurons (Stemkowski et al., 2015). In most cases, neurons were pretreated with 50 ng/ml glial cell line derived neurotrophic factor (GDNF; Alomone Labs, Jerusalem, Israel; prepared in 0.1% BSA (Sigma) dissolved in HBSS) following the initial DRG isolation (Day 0) cells (Fig. 1a). After 3d in culture with GDNF, dishes were divided into 2 groups, both of which received continued supplementation with 50 ng/ml GDNF. IL-1β was applied for the following 5–6 d in defined medium supplemented with 50 ng/ml GDNF. These protocols were also applied to neurons receiving 50 ng/ml NGF (Nerve Growth Factor, Alomone Labs, Jerusalem, Israel) instead of GDNF (Fig. 1a).

2.3. Classification of DRG neurons

DRG neurons were classified according to soma diameter as 'small' (< 30 μm), 'medium' (30–40 μm), or 'large' (> 40 μm) as measured with a calibrated micrometer in the eye piece of a Nikon TE300 inverted fluorescence microscope (Stemkowski et al., 2015; Stemkowski and Smith, 2012a). Since small diameter IB_4-positive and IB_4-negative sensory neurons are functionally distinct with regard to pain physiology (Stucky and Lewin, 1999; Fang et al., 2006), these cell types were distinguished by including IB_4 Alexa Fluor® 488 conjugate (Invitrogen, Eugene, OR, USA) isolectin B4 (5 μg/ml) in dishes of DRG neurons for 10 min prior to recording. IB_4-positive (IB_4^+) neurons displayed green fluorescence (Silverman and Kruger, 1990). To limit misclassification of small IB_4-negative (IB_4^-) or possibly peptidergic visceral DRG neurons as small IB_4^+, only the most intensely stained small DRG neurons were considered IB_4^+(Robinson et al., 2004). A photomicrograph of $IB4^+$ neurons is shown in Fig. 1b. In this image only the two brightyly satined small neurons would be selected for recording.

2.4. Electrophysiology

Whole-cell recordings were made at room temperature (22 °C) from small IB_4-positive neurons using a NPI SEC-05LX amplifier (ALA Scientific Instruments Farmingdale NY, USA) in either bridge-balance current-clamp mode or discontinuous single-electrode current or voltage-clamp mode. The effectiveness of the voltage-clamp was confirmed by examining voltage recordings from neurons and discarding recordings where the voltage trace was slow to rise or distorted. Input capacitance (C_{in}) was calculated from the membrane time constant and input resistance or by the integration of the capacitative transient generated by a 10 mV voltage step (Abdulla and Smith, 1997). Current records were low pass filtered to -3 dB at 300 Hz.

For current-clamp experiments, external solution contained (in mM) 127 NaCl, 2.5 KCl, 1.2 NaH_2PO_4, 26 $NaHCO_3$, 2.5 $CaCl_2$, 1.3 $MgSO_4$ and 25 D-glucose saturated with 95% O_2–5% CO_2. Internal (pipette) solution contained (in mM) 130 KGluconate, 4 Mg-ATP, 0.3 Na-GTP, 10 EGTA, 2 $CaCl_2$ and 10 HEPES (adjusted to pH 7.2 with KOH; osmolarity 310–320 mOsm). Recording electrodes had resistances of 2–5 MΩ). Action potentials were generated with 5 ms depolarizing current pulses while the resting membrane potential was adjusted to -60 mV. AP duration was measured at 50% AP amplitude (Spike Height; Fig. 1c) using APs generated with rheobase current strength. Rheobase was determined by injection of a series of depolarizing current commands in 0.1 nA increments. The first current amplitude that produced an AP was noted. This method meant that rheobase data had to be analyzed by non-parametric statistics.

I_{Na} was recorded in an external solution containing (in mM), 75 TEA−Cl, 50 NaCl, 5 KCl, 4 $MgCl_2$, 10 HEPES and 60 D-glucose (adjusted to pH 7.4 with NaOH; osmolarity 330 mOsm). The relatively low concentration of extracellular Na^+ was used to reduce I_{Na} amplitude and to thereby facilitate clamp fidelity. Internal solution contained (in mM), 140 CsCl, 10 NaCl, 2 MgATP, 0.3 Na_2GTP, 2 EGTA, 10 HEPES and 2 $MgCl_2$ (adjusted to pH 7.2 with NaOH; osmolarity 300–310 mOsm). Tetrodotoxin (TTX) (Alomone Labs, Jerusalem, Israel) (300 nM) was applied by superfusion. Total I_{Na} was recorded in response to 40 ms depolarizing voltage commands from a holding potential (V_h = −90 mV) and leak subtracted by means of a p/4 protocol (Stemkowski et al., 2015). Current remaining following treatment with 300 nM TTX was defined as TTX-resistant (TTX-R I_{Na}) and digital subtraction of these recordings from total I_{Na} revealed TTX-sensitive I_{Na} (TTX-S I_{Na} see Fig. 5a–c).

Current decay (fast inactivation) was fitted with a single exponent function, $f(t) = \Sigma_{i=1}^{n} Ai\ e^{-t/\tau i} + C$. For voltage-dependence of activation, normalized (I/I_{-20}) I-V curves were fit with a single Boltzmann function, y = A2 + (A1-A2)/(1 + exp.((x-x_0)/dx)) which yielded slope factor and voltage for half activation (V_{50}). I_{Na} steady-state fast inactivation protocol involved 300 ms prepulses increasing from −110 mV followed by 10 ms test pulses to -10 mV to determine the fraction of current available (I/I_{-110}). The I_{Na} steady-state slow inactivation protocol involved application of 5 s prepulses, followed by 20 ms recovery pulses to -120 mV (to allow recovery from fast inactivation), followed by 10 ms test pulses to -10 mV to determine the fraction of current available ($I/I - 120$).

For recording K^+ channel currents, external solution contained (in mM) 145 *N*-methyl-D-glucamine (NMG)Cl, 10 KCl, 2.5 $CaCl_2$, 10 HEPES, 1.0 $MgCl_2$ and 10 D-glucose (adjusted to pH 7.4 with HCl; 320 mosm). The relatively high concentration of extracellular K^+ was used to reduce I_K amplitude and to thereby facilitate clamp fidelity. Internal solution contained (in mM) 100 K gluconate, 40 NMG−Cl, 2 Mg-ATP, 0.3 Na_2GTP, 11 EGTA, 10 HEPES and 0.1 $CaCl_2$ (adjusted to pH 7.2 with HCl; 300 mosm; E_K = -58 mV). In view of the complexity and variability of potassium currents in DRG neurons (Gold et al., 1996) a simplified approach was used for their isolation (Abdulla and Smith, 2001b; Stemkowski et al., 2015). Total I_K was recorded at voltages between −60 mV and + 60 mV following a 500 ms conditioning

prepulse to −120 mV or − 30 mV and leak subtracted by means of a p/6 protocol. Voltage commands were then repeated in the presence of 5 mM Mn^{2+} to reveal Mn^{2+} resistant I_K. Digital subtraction of Mn^{2+}-resistant I_K from the total I_K yielded Mn^{2+} sensitive I_K which corresponded to the total Ca^{2+} sensitive K^+ current ($I_{K,Ca}$) and the underlying conductance ($g_{K,Ca}$) (Abdulla and Smith, 2001b). As is discussed below, this current is thought to be carried by high conductance, voltage and Ca^{2+} sensitive K^+ channels, (*i.e* BK(Ca) channels. Detection of I_A involved subtracting Mn^{2+} resistant I_K recorded following a − 30 mV prepulse from that recorded following a − 120 mV prepulse (Stemkowski et al., 2015). Mn2+ resistant IK recorded from -30 mV was assumed to reflect delayed rectifier current (I_{DR}).

I_{Ca} was measured using Ba^{2+} as a charge carrier (I_{Ba}). External solution contained (in mM) 160 TEA−Cl, 10 HEPES, 2 $BaCl_2$, 10 D-glucose and 300 nM TTX (adjusted to pH 7.4 with TEA-OH; osmolarity 330–340 mOsm). Internal solution contained (in mM) 120 CsCl, 5 Mg-ATP, 0.4 Na_2-GTP, 10 EGTA and 20 HEPES (adjusted to pH 7.2 with CsOH; osmolarity 300–310 mOsm). I_{Ba} was evoked using a series of 150 ms depolarizing voltage commands from $V_h = -100$ mV or $V_h = -60$ mV and leak subtracted by means of a p/6 protocol. For the voltage-dependence of I_{Ba} inactivation, the fraction of current available at $V_{cmd} = -10$ mV was determined in response to a series of 3.5 s incremental prepulses from $V_h = -100$ mV. Normalized (I/I_{-110}) inactivation curves were fit with a single Boltzmann function, $y = A2 + (A1-A2)/(1 + \exp((x-x_0)/dx))$.

2.5. Drugs and chemicals

Unless stated otherwise, all reagents were from SigmaAldrich Canada. Iberotoxin (IBTX), Nerve Growth Factor (NGF) and GDNF were from Alomone Laboratories (Jerusalem Israel).

2.6. Analysis and statistics

All electrophysiological data were acquired and analyzed using pCLAMP 10 software (Axon Instruments). Figures were produced with Origin 2018 (Origin Lab, Northampton, MA, USA) and/or Graphpad Prism. Where applicable, data are presented as mean ± standard error of mean (s.e.m.). Statistical comparisons were made using unpaired, two tailed Student's *t*-test for AP parameters and multiple unpaired Student's t-test with Holm-Sidak post hoc test for currents. Non parametric Mann-Whitney test for non-parametric values. *P* values from these statistical tests were determined using GraphPad Prism 5.00 (GraphPad Software, San Diego, CA, USA).

3. Results

3.1. Persistent effect of IL-1β on action potential duration

In our previous study, the excitability of small $IB4^+$ neurons was only slightly increased by 5-6d exposure to IL-1β, whereas the alterations to AP waveform were far more noticeable These experiments were done in defined medium, neurotrophin-free media. Under these conditions, IL-1β increased AP duration by 35% (Stemkowski and Smith, 2012a).

It is well established however that glial cell line derived neurotrophic factor (GDNF) is required for the maintenance of $Na_v1.8$ channels and the general neurotrophic support of IB_4^+ DRG neurons (Fjell et al., 1999; Cummins et al., 2000; Zwick et al., 2002; Golden et al., 2010). Since GDNF and IL-1β share various downstream effector proteins such as MAPK/ERK (Bogen et al., 2008; MacGillivray et al., 2000; Lu et al., 2005), we wondered whether the cytokine would still increase AP duration in IB_4^+ neurons that had access to the normal neurotrophic support of GDNF.

Fig. 2a shows that inclusion of GDNF in the defined medium increased AP duration (spike width) in small $IB4^+$ neurons from 2.13 ± 0.14 ms ($n = 25$) to 2.67 ± 0.15 ms ($n = 35$; $p < 0.01$). 5-6d treatment of cells that had been maintained in in GDNF with IL-1β produced a further increase in AP duration to 3.39 ± 0.17 ms ($n = 34$, $p < 0.01$;Fig. 2b).

Fig. 2c shows averaged recordings of APs in 35 GDNF treated and 34 GDNF + IL-1β treated small, $IB4^+$ neurons. AP amplitude and duration are clearly increased by exposure to IL-1β. Unless otherwise stated, all data presented below were obtained from GDNF treated neurons.

Since the ability of IL-1β to increase the excitability of medium sized DRG is reversible (Stemkowski et al., 2015) we wondered whether this was also the case for the increase in AP duration in small $IB4^+$ neurons. Interestingly, this effect of IL-1β was not reversed following incubation of the cultures for 3–4 days in cytokine-free GDNF medium. Thus AP duration of IB_4^+ neurons which had been exposed to IL-1β for 5-6d prior to 3-4d of cytokine washout was 4.36 ± 0.23 ($n = 32$). This was significantly greater than the AP duration observed in time matched controls (3.56 ± 0.17 ms; n = 35; $p < 0.007$; Fig. 2d).

Fig. 2e shows averaged recordings of action potentials in 32 neurons that were maintained in the presence of GDNF and exposed to IL-1β for 5-6d followed by a 3-4d washout period in cytokine free medium (IL-1β wash). These are compared with averaged recordings from neurons that were maintained in GDNF but were never exposed to cytokine. Error bars (showing SEM) are shown in one direction to show the persistent increase in AP amplitude and duration following 3-4d washout of IL-β.

Classically, IB_4^+ neurons express rearranged during transfection (RET) receptors for GDNF but lack tropomyosin related kinase A (TrkA) receptors for NGF (Molliver et al., 1995; Molliver et al., 1997; Hunt and Mantyh, 2001). However, more recent studies indicate that 35% of IB_4^+ neurons also express TrkA (Fang et al., 2006). NGF treatment increased AP duration from 2.13 ± 0.14 ms ($n = 21$) to 2.81 ± 0.26 ms ($n = 24$; Fig. 2f; $p < 0.05$). Treatment of cells maintained in NGF with IL-1β produced an additional increase in AP duration to 4.47 ± 0.59 (n = 24 $p < 0.015$, Fig. 2g).

3.2. Effects of IL-1β on AP amplitude and other action potential parameters

Although the irreversible increase in AP duration is the most obvious effect of IL-1β in GDNF- treated neurons, there were significant changes in other AP parameters. IL-1β increased AP amplitude (Fig. 3a), decreased rheobase (Fig. 3b), increased maximum rate of rise of the upshot of the AP (Fig. 3c), decreased maximum rate of AP decay (Fig. 3d), increased time to peak of AHP (Fig. 3e) but did not affect AHP amplitude (Fig. 3f).

3.3. Parameter specific reversibility of IL-1β effects

Unlike the irreversible increase in AP duration (spike width, Fig. 2b–e), changes in AP amplitude (spike height, Fig. 4a), rheobase (Fig. 4b) and AHP time to peak (Fig. 4e) appeared to recover following IL-1β washout. The values of these parameters in neurons that had been exposed to cytokine for 5-6d followed by 3-4d washout were not different from time controls. By contrast, changes in maximum rate of rise and decay of AP's seemed to persist even after IL-1β was removed (Fig. 4c and d). As seen during 5-6d IL-1β exposure (Fig. 3f) there was no difference in AHP amplitude following 5–6 days IL-1β exposure and 3–4 days washout compared to time control (Fig. 4f). Our findings on the reversibility of the various actions of IL-1β are summarized in Table 1.

3.4. Effects of long-term IL-1β exposure on total, TTX-R and TTX-S I_{Na}

To understand the mechanisms underlying IL-1β-induced changes in AP shape, we carried out a voltage-clamp analysis of its actions on the voltage gated Na+, Ca2+ and K+ channels found in small IB_4-positive neurons Total I_{Na} density was recorded using a series of depolarizing voltage commands from $V_h = -90$ mV (Fig. 5a). Neurons were then

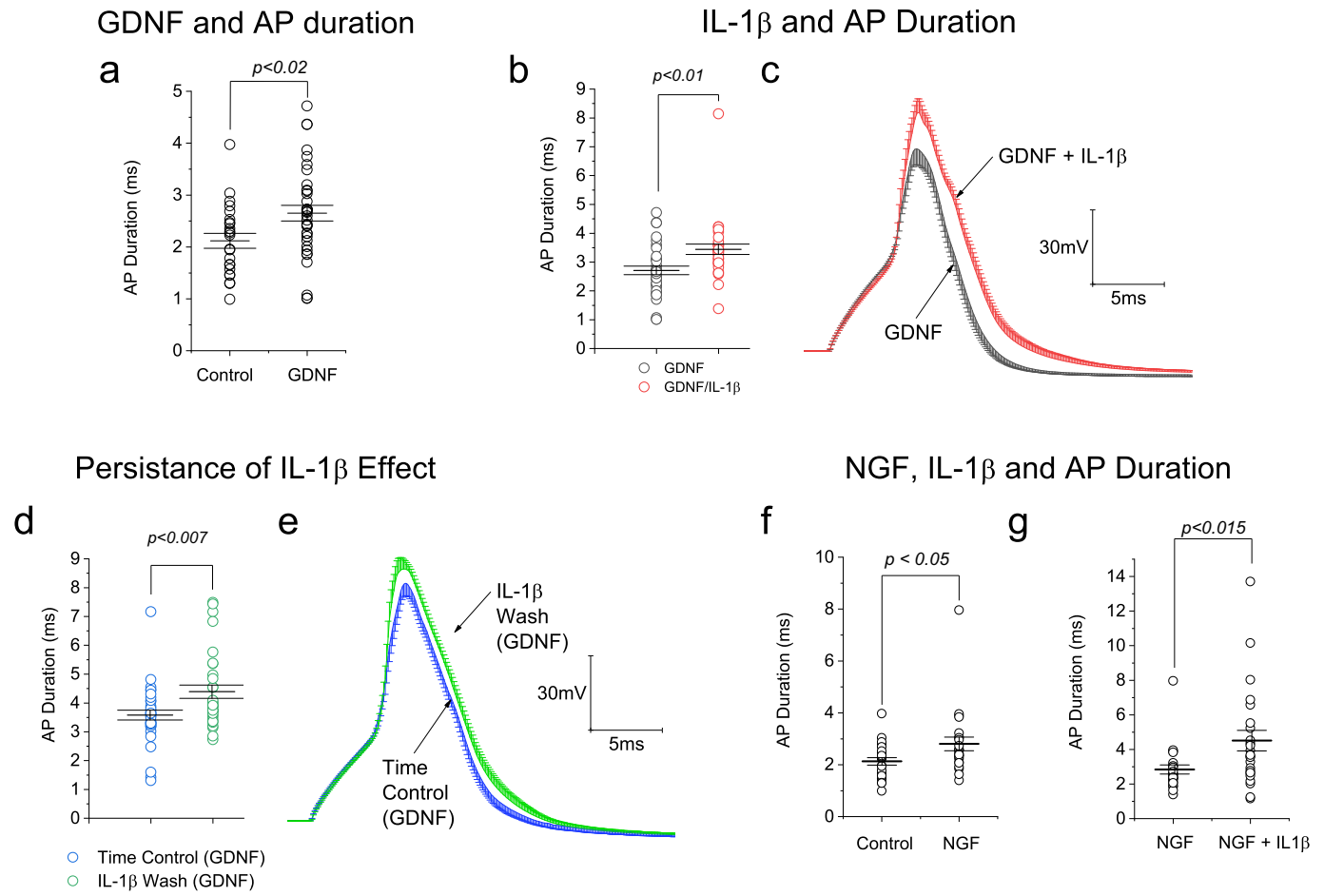

Fig. 2. a. Graph to show effect of GDNF on AP duration. On this and all similar graphs, bold lines show mean value and error bars show SEM. **b.** Graph to show increase in AP duration produced by exposure of GDNF treated neurons to IL1β for 5–6 days. **c.** Averaged recordings from 35 GDNF treated neurons and 34 GDNF neurons exposed to IL-1β for 5–6 days. Error bars shown in upward direction only show SEM. **d.** Graph to show persistance of IL-1β effect. IL-1β wash data is from neurons that were exposed to IL-1β for 5–6 days but not studied until 3–4 days after IL-1β washout. **e.** Averaged recordings obtained from 35 GDNF treated neurons 3–4 days after 5–6 days exposure to IL-1β. These are compared to time control neurons that were exposed to GDNF for 12–14 days (see Fig. 1a). **f.** Graph to show effect of NGF on AP duration. **g.** Graph to show increase in AP duration produced by exposure of NGF treated neurons to IL1β for 5–6 days.

treated with 300 nM TTX to isolate TTX-sensitive (TTX-S) I_{Na} from TTX-resistant (TTX-R) I_{Na} (Fig. 5b). Digital subtraction (Fig. 5c) reveals TTX-S I_{Na}.

The importance of GDNF in maintaining Na_v 1.8 and Na_v 1.9 in DRG neurons (Fjell et al., 1999) underlines the need to include it in continued analyses of effects of IL-1β on cation currents. The averaged I-V plots in Fig. 5d indicate that addition of IL-1β to GDNF treated cultures produced highly significant increases in total I_{Na} density ($p < 0.001$ at −40, −30 and -20 mV; *t*-test; $n = 19$). By contrast, TTX-R I_{Na} density, which was recorded in the presence of 300 nM TTX, was unaffected (Fig. 5e; n = 19 for control, $n = 18$ for IL-1β). It is therefore likely that the increase in total I_{Na} reflects an action on TTX-S I_{Na} density. This is illustrated in the current voltage plots shown in Fig. 5f where IL-1β produces highly significant increases in the density of TTX-S I_{Na} ($p < 0.001$ between −40 and 0 mV; t-test; n = 18).

Fig. 5g–i illustrate the effects of IL-1β on voltage-dependence of activation for total, TTX-R and TTX-S g_{Na}. Findings are summarized in Table 2. Fig. 5g shows that addition of IL-1β to GDNF treated cultures shifts the activation curve for total g_{Na} towards more hyperpolarized potentials. This is reflected in a significant change in the V_{50} ($p < 0.0001$) but not the slope factor ($p > 0.6$, Table 2). The activation curve for TTX-R g_{Na} was unchanged (for V_{50}, $p > 0.2$ for slope factor $p > 0.8$, Table 2, Fig. 5h). Changes in TTX-S g_{Na} were slightly different from those seen in total g_{Na}. Although the activation curve was shifted towards more negative voltages (Fig. 5i), V_{50} was also significantly changed ($p < 0.0001$, Table 2), slope factor was unchanged ($p > 0.75$).

3.5. Effects of long-term IL-1β exposure on inactivation of total, TTX-R and TTX-S g_{Na}

Long-term IL-1β treatment also lead to modest but significant changes in steady-state fast inactivation (Table 2). For total g_{Na}, IL-1β treatment lead to a hyperpolarizing shift in the inactivation curve, (Fig. 5g) which was accompanied by significant change in V_{50} ($p < 0.005$) and slope factor ($p < 0.03$; Table 2). For TTX-R g_{Na}, (Fig. 5h) the inactivation V_{50} changed from −28.29 ± 0.42 mV to −26.77 ± 0.37 mV ($p < 0.05$), but slope factor was unchanged ($p > 0.13$; Table 2). Changes in the TTX-S g_{Na} inactivation were slightly different from those seen with total g_{Na} inactivation. Although the slope factor was significantly changed by IL-1β treatment ($p < 0.006$); the V_{50} was unaffected (Fig. 5i and Table 2).

Since shifts in the voltage-dependence of steady-state *slow* inactivation have been previously reported for I_{Na} in the context of pain hypersensitivity (Choi et al., 2007; Waxman and Zamponi, 2014; Binshtok et al., 2008), 5 s prepulses, followed by 20 ms recovery pulses to −120 mV (to allow recovery from fast inactivation), preceded 1 ms test pulses to −10 mV to determine the fraction of current available. As indicated from overlapping steady-state *slow* inactivation curves (Fig. 5j and k), addition of IL-1β to GDNF treated neurons failed to affect slow

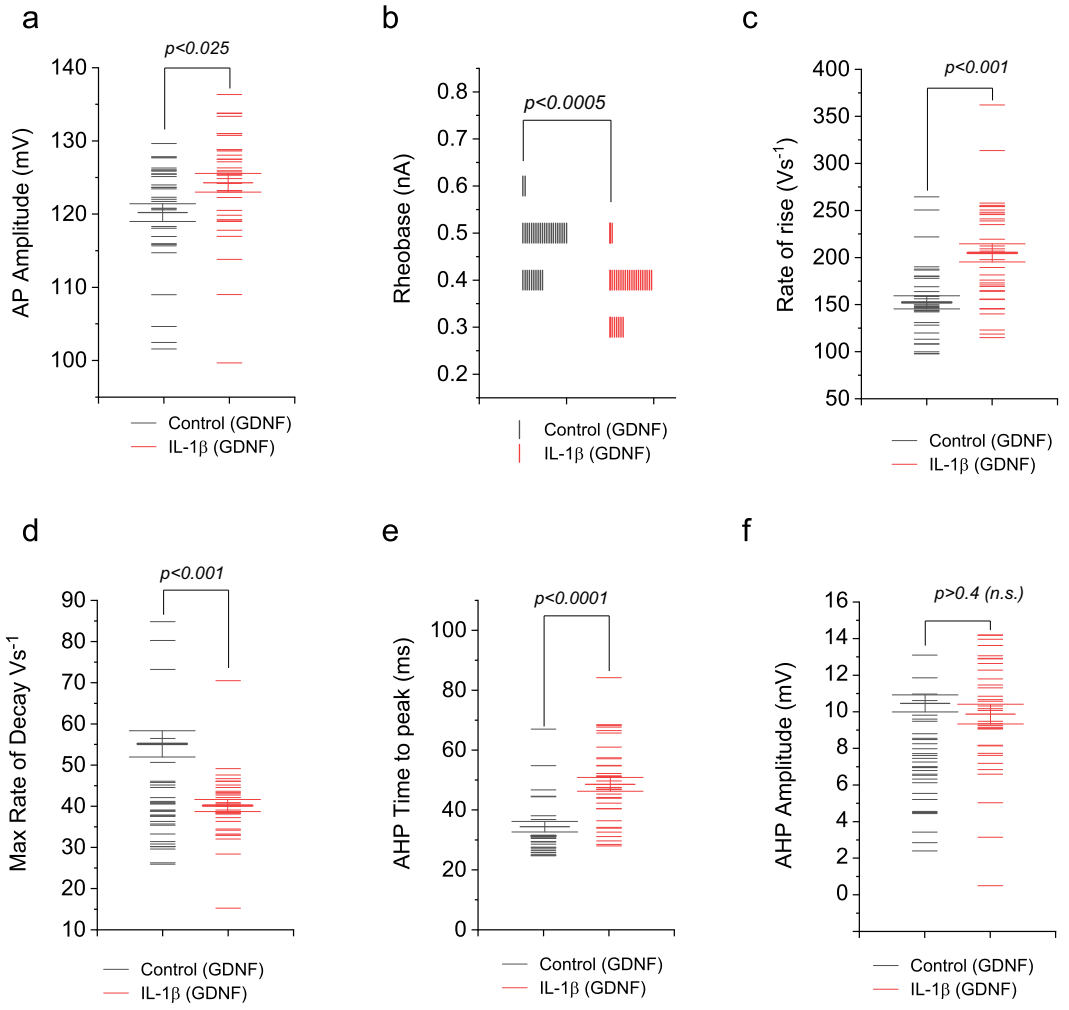

Fig. 3. Graphs to show effect of exposure of GDNF-treated neurons to IL-1β for 5-6d. AP amplitude is increased (**a**), rheobase is reduced (**b**), rate of rise of AP is increased (**c**), Maximum rate of AP decay is decreased (**d**), AHP time to peak is increased (**e**) but AHP amplitude is unchanged (**f**).

inactivation.

The significant increase in AP duration in small IB_4-positive neurons after IL-1β treatment (Fig. 2b and c) could also be associated with slowed *rates* of g_{Na} inactivation (Snape et al., 2009). This not seem to be the case as fast inactivation time constants for total and TTX-R I_{Na} were unchanged by IL-1β (Fig. 5l and m).

3.6. Effects of long-term IL-1β exposure on K^+ channel currents

Voltage-clamp protocols and solutions were designed to examine voltage-dependent K^+ currents as well as voltage and Ca^{2+}-dependent K^+ current ($I_{K,Ca}$) and A-currents. We recorded total I_K and Mn^{2+}-resistant I_K, and obtained Mn^{2+}-sensitive I_K which was measure of $I_{K,Ca}$ and I_A by subtraction and/or by using two different holding potentials (V_h) (Stemkowski et al., 2015). Fig. 6a *i)* illustrates a family of total I_K evoked by a series of depolarizing voltage commands from −120 mV. Fig. 6a *ii)* illustrates Mn^{2+}-resistant I_K recorded in the same neuron in the presence of 5 mM Mn^{2+}. Fig. 6a *iii)* is the subtraction of records in Fig. 6a *ii)* from those in Fig. 6a *i)* to reveal Mn^{2+}-sensitive I_K, ($I_{K,Ca}$). Fig. 6b *i)* illustrates Mn^{2+}-resistant I_K recorded from −120 mV in another IB_4^+ neuron and Fig. 6b *ii)* illustrates Mn^{2+}-resistant currents recorded in the same neuron from V_h = −30 mV. This is thought to represent delayed rectifier type K^+ currents (I_{DR}). Subtraction of recordings in Fig. 6b *ii)* from those in Fig. 6b *i)* reveals a rapidly activating/rapidly inactivating current (Fig. 6b *iii*), that likely reflects activation of multiple channel types including Kv4.1 and Kv4.3 (Yunoki et al., 2014; Gold et al., 1996). In agreement with this, we found considerable variation in the rate of current inactivation in the cells studied. We have defined "I_A" as that which shown clear inactivation within the first 100 ms of a voltage command (Fig. 6c *iii*). According to this definition, 5/19 GDNF treated neurons expressed I_A compared to 7/18 neurons in GDNF plus IL-1β.

By contrast with its strong effects on K^+ currents in medium sized DRG neurons (Stemkowski et al., 2015), IL-1*β* produced only modest effects in IB_4^+ neurons. Neither the densities of total I_K (from V_h = -120 mV, Fig. 6c), nor Mn^{2+}- resistant I_K (from V_h = -30 mV, Fig. 6d; presumed I_{DR}) nor "I_A" (Fig. 6e) were altered. There was however a noticeable reduction of $I_{K,Ca}$ which was significant at voltages positive to +20 mV. For example, IL-1β reduced current density from 70.6 ± 6.15 pA.pF^{-1}, n = 17 to 44.5 ± 8.04 pA.pF^{-1}, n = 16 at +60 mV ($p < 0.02$ unpaired *t*-test, Fig. 6f); This represents a 37% reduction or a 26 pA.pF^{-1} change in I_{KCa}. Since total I_K at +60 mV is about ~ 200pA.pf^{-1} (Fig. 6c), this small change in $I_{K,Ca}$ density is not reflected as a statistically significant change in the density of the total current.

3.7. Effects of long-term IL-1β exposure on Ca^{2+} channel currents

Typical recordings of Ca^{2+} channel currents evoked by a series of 150 ms depolarizing voltage commands using Ba^{2+} as the charge carrier (I_{Ba}) are shown in Fig. 7a. Total currents from a holding potential of -100 mV were unaffected by addition of IL-1β to neurons maintained in

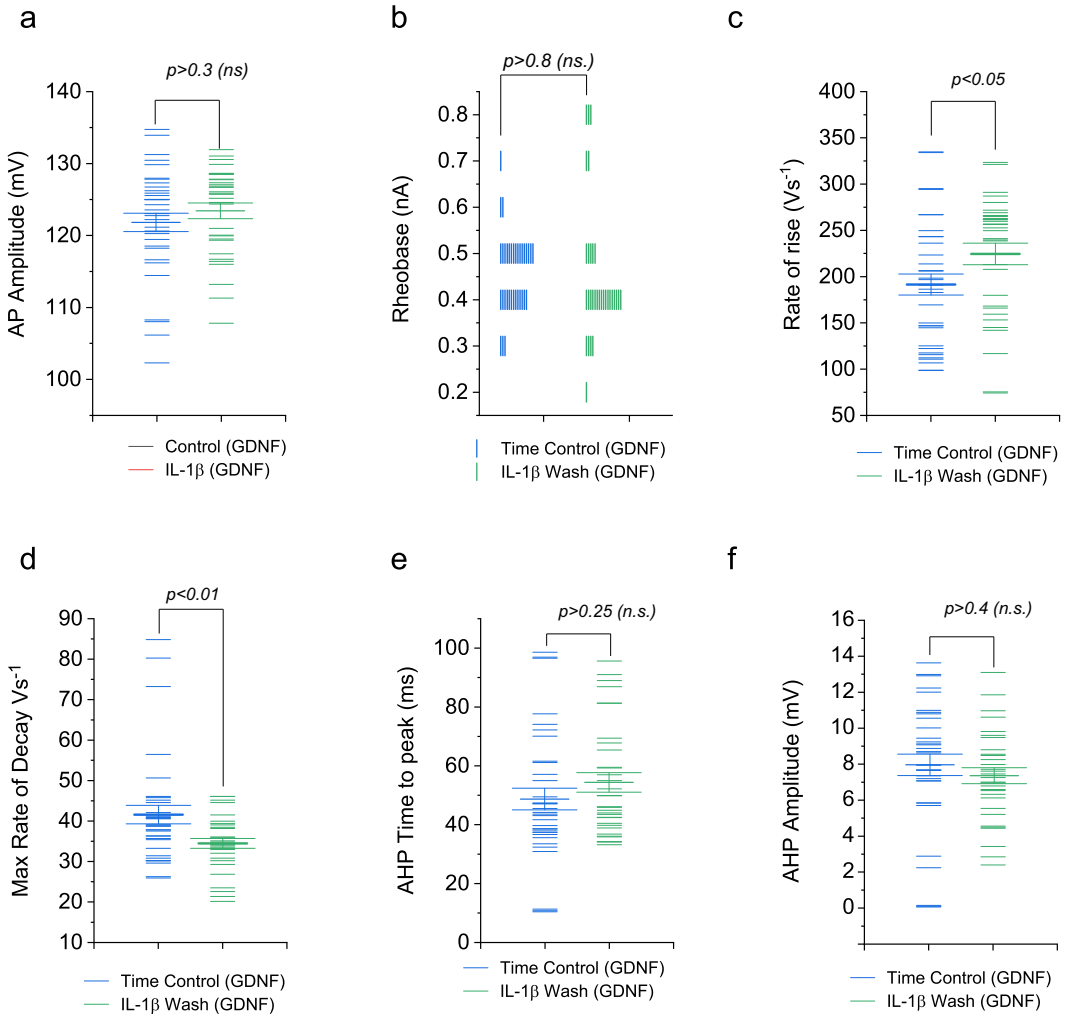

Fig. 4. Graphs to show data from GDNF neurons obtained 3–4 days after 5–6 days exposure to IL-1β compared to time control (12–14 days exposure to GDNF alone). AP Amplitude and rheobase are not different from time controls, indicating effects of IL1β is reversed (**a** and **b**). Rate of rise and maximum rate of decay of AP are significantly different from time controls, indicating lasting effect of IL-1β (**c** and **d**). Time to peak of AHP is not different from time controls indicating another reversible action of IL-1β (**e**), AHP amplitude remains unchanged (**f**).

Table 1
Effects of IL-1β on AP parameters.

	Effect of IL-1β	Reversible	Conductance or current affected
AP duration	↑	No	$g_{K\text{-}Ca}$/BK(Ca)
AP amplitude	↑	Yes	TTX-S I_{Na}
Rheobase	↓	Yes	TTX-S I_{Na}
Rate of rise	↑	No	TTX-S I_{Na}
Rate of decay	↓	No	$g_{K\text{-}Ca}$/BK(Ca)
AHP time to peak	↑	Yes	?
AHP amplitude	↔	N/A	N/A

GDNF (Fig. 7b). This included currents activated at -40 mV which are dominated by T-type I_{Ca}. Since peripheral nerve injury has been reported to increase inactivation of Ba^{2+}conductances (Baccei and Kocsis, 2000; Abdulla and Smith, 2001b), the possibility that long-term exposure to IL-1β affects I_{Ba} inactivation might be reflected as a decrease in I_{Ba} recorded from -60 mV; close to the normal resting potential of DRG neurons. However, this did not appear to be the case because IL-1β failed to affect I_{Ba} recorded at this voltage (Fig. 7c).

Since APs recorded from GDNF/IL-1β treated neurons are of longer duration and higher amplitude than those in control GDNF treated neurons (Fig. 2) the voltage trajectory encountered by Ca^{2+} channels in the two situations may result in altered Ca^{2+} influx. To test this, we designed voltage command waveforms that would mimic APs in GDNF treated neurons and in GDNF/IL-1β treated neurons and used them to generate I_{Ba} (Fig. 7d). A control neuron was first exposed to a voltage protocol mimicking a control (GDNF) AP and then to a voltage protocol mimicking the longer duration and greater amplitude AP as found in the presence of GDNF and IL-1β. Fig. 7e shows that maximal I_{Ba} flows during and after the AP repolarization and the AP voltage trajectory expected from an GDNF/IL-1β treated neuron evokes more I_{Ba} than that modeled from a GDNF treated neuron.

3.8. $I_{K,Ca}$ and IL-1β – induced increases in AP duration

Although other K^+ currents are little affected (Fig. 6c–e), $I_{K,Ca}$ is reduced by 37% by IL-1β (Fig. 6f). To test the possibility that this contributes to the increase in AP duration (Fig. 2), we examined the effect of the BK(Ca) channel blocker iberotoxin (IBTX; 100 nM) on AP's from GDNF treated and GDNF/IL-1β treated neurons. Whereas IBTX increased AP duration in GDNF treated neurons to 225.1 ± 23.5% of control (n = 7; Fig. 7f and h) it had less effect on GDNF/IL-1β treated neurons (Fig. 7g and h) where it increased AP duration to only 154.3 ± 17.6 of control (n = 8). The difference in percentage changes in AP duration in each situation was significant ($p < 0.05$; Fig. 7h). The weaker effect of IBTX in the presence of IL-1β (Fig. 7f–h) suggests

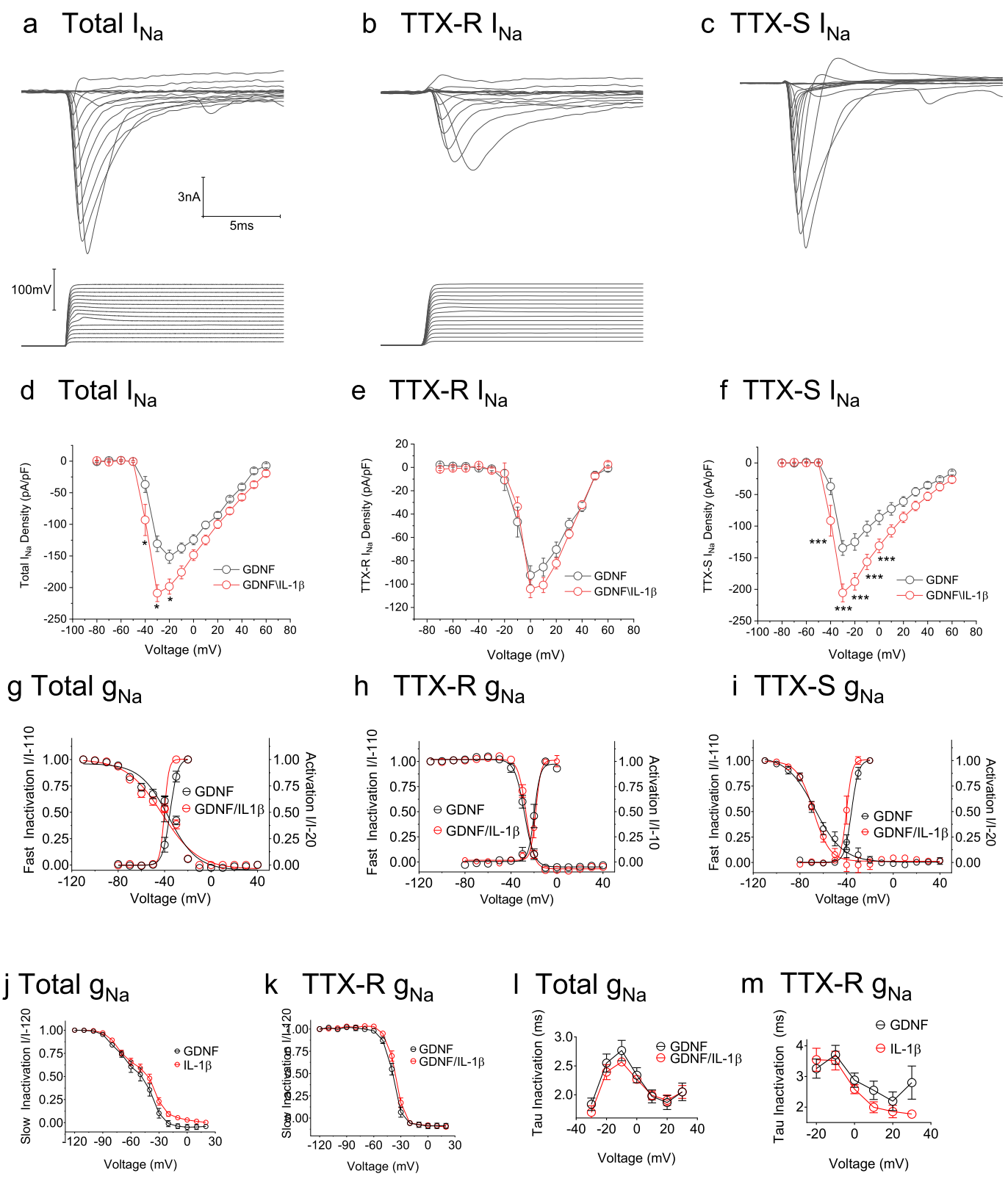

Fig. 5. Effects of IL-1β on I_{Na}. **a.** Typical recordings of total I_{Na} from a GDNF treated small IB_4^+ neuron. **b.** TTX-R I_{Na} in the same neuron recorded in the presence of 300 nM TTX. **c.** TTX-S I_{Na} obtained by subtraction of recordings in **b** from those in **a. d,e** and **f.** Current-voltage plots for total, TTX-R and TTX-S I_{Na} obtained from 19 GDNF treated neurons and 18 GDNF neurons following 5-6d exposure to IL-1β. Total and TTX-S I_{Na} are increased by IL-1β but TTX-R I_{Na} is unaffected. **g,h** and **i.** Activation and inactivation plots for total, TTX-R and TTX-S g_{Na} obtained from GDNF treated neurons and GDNF neurons following 5-6d exposure to IL-1β. (n's range from 14 for inactivation of TTX-S g_{Na} in GDNF treated cells (**i**) to 21 for inactivation of total g_{Na} in GDNF treated neurons (**g** see Table 2). **j** and **k** Slow inactivation plots for total g_{Na} and TTX-R g_{Na} in in the presence and absence of IL-1β. Total g_{Na} inactivation, $n = 20$ in GDNF, $n = 18$ in GDNF + IL-1β. TTX-R g_{Na} inactivation, $n = 15$ in GDNF, $n = 16$ in GDNF + IL-1β.**l** and **m.** Voltage dependence of time constant of inactivation (τ) for total g_{Na} and TTX-R g_{Na} in GDNF treated neurons in presence or absence of IL-1β. τ for total g_{Na} inactivation, n = 20 in GDNF, n = 18 in GDNF + IL-1β.τ for TTX-R g_{Na} inactivation, n = 15 in GDNF, n = 16 in GDNF + IL-1β. Error bars indicate SEM.*** = $p < 0.001$.

Table 2
Effects of IL-1β on Na^+ channel currents.

	Control (GDNF)	IL-1β (GDNF)
Total g_{Na} activation V_{50}	−35.26 ± 0.7021 (20)	−40.21 ± 0.4599 (19) $p < 0.0001$***
TTX-R g_{Na} activation V_{50}	−19.74 ± 0.6089 (18)	−18.35 ± 1.005 (17) $p = 0.2393$
TTX-S g_{Na} activation V_{50}	−35.76 ± 0.7912 (18)	−40.11 ± 0.5841 (16) $p = 0.0001$***
Total g_{Na} activation slope factor	3.299 ± 0.4205 (20)	1.932 ± 2.626 (19) $p = 0.6013$
TTX-R g_{Na} activation slope factor	2.59 ± 1.448 (18)	2.238 ± 1.167 (17) $p = 0.8521$
TTX-S g_{Na} activation slope factor	2.992 ± 0.4558 (18)	2.442 ± 1.777 (16) $p = 0.7541$
Total g_{Na} fast inactivation V_{50}	−36.70 ± 0.98 (21)	−41.97 ± 1.13 (18) $p = 0.0011$
TTX-R g_{Na} fast inactivation V_{50}	−28.29 ± 0.416 (18)	−26.77 ± 0.3668 (17) $p = 0.0101$
TTX-S g_{Na} fast inactivation V_{50}	−67.08 ± 1.832 (14)	−68.37 ± 0.9757 (16) $p = 0.5249$
Total g_{Na} fast inactivation slope factor	−12.25 ± 0.8957 (21)	−15.49 ± 1.075 (18) $p = 0.0251$
TTX-R g_{Na} fast inactivation slope factor	−4.21 ± 0.3894 (18)	−3.473 ± 0.2795 (17) $p = 0.1375$
TTX-S g_{Na} Fast Inactivation Slope Factor	−12.02 ± 1.541 (14)	−6.962 ± 0.8444 (16) $p = 0.0059$

that fewer functional BK(Ca) channels were available in cytokine treated neurons. This attenuation may therefore play a role in the IL-1β induced increase in AP duration.

4. Discussion

4.1. Ion channels and conductances affected by IL-1β

We have shown previously that exposure of small $IB4^+$ neurons to IL-1β for 5-6d in defined medium, neurotrophin-free cultures results in a marked increase in AP duration and that this effect is mediated via IL-1R (Stemkowski and Smith, 2012a). Since the maintenance of various cation conductances, notably TTX-resistant $Na_v1.8$ in small DRG neurons is dependent on appropriate neurotrophic support (Fjell et al., 1999; Cummins et al., 2000; Zwick et al., 2002; Golden et al., 2010), we have re-examined the effect of IL-1β on GDNF treated small $IB4^+$ neurons. As was seen in previous experiments on neurotophin-free defined medium cultures (Stemkowski and Smith, 2012a), IL-1β produced a significant increase in AP duration and decreased the rate of AP repolarisation in GDNF treated neurons (Fig. 2b and 3d). Although AHP amplitude was unaffected in both situations (Fig. 3f), the increase in spike height (Fig. 3a) and rate of AP rise (Fig. 3c) and decrease in rheobase (Fig. 3b) seen in response to IL-1β in GDNF treated neurons was not seen previously in neurons maintained in neurotrophin-free defined media (Stemkowski and Smith, 2012a).

In view of reports that 35% of $IB4^+$ neurons also express TrkA (Fang et al., 2006), we examined the effect of IL-1β in the presence of NGF. As in GDNF treated neurons, IL-1β also increased AP duration in NGF treated neurons (Fig. 2g).

The cation channels most profoundly affected by IL-1β in GDNF treated small IB_4^+ neurons included TTX-S Na^+ channels (Fig. 5c) and $I_{K,Ca}$ channels (Fig. 6f). In view of their voltage-dependence (Fig. 6f) and the actions of IBTX (Fig. 7f) these were likely BK(Ca) (K_{Ca} 1.1) channels. This contrasts with the situation in medium sized DRG neurons where sodium currents were affected only modestly and the amplitudes of A-current and delayed rectifier currents were reduced by 68% and 64% respectively (Stemkowski et al., 2015). The increase in TTX-S I_{Na} and the shift of its activation curve to more negative potentials (Fig. 5i and Table 2) likely contribiues to the increased AP amplitude. These effects override changes in inactivation as IL-1β moves inactivation curves to more negative potentials. This decreases g_{Na} availability at resting poential (-60 mV, Fig. 5g). Moreover, decreases in the rate of inactivation are not seen (Fig. 5m), so this also does not contibute to the cytokine-induced increase in AP duration.

Since g_{KCa} is the only K^+ conductance altered by IL-1β (Fig. 6), a reduction in this conductance which we have attributed to BK(Ca) channels likely contributes to increased AP duration. This idea is supported by the observation that AP duration in cells treated with IL-1β is less sensitive to the BK(Ca) blocker IBTX (Fig. 7h). Changes in BK(Ca) are not secondary to reduced Ca^{2+} influx as I_{Ba} is unaffected by IL-1β (Fig. 7b and c). The current voltage plot in Fig. 7b also shows that IL-1β failed to affect currents recorded at -40 mV which would mainly represent T-type Ca^{2+} channel currents.

The lack of effect of long term IL-1β exposure on TTX-R I_{Na} was somewhat unexpected as Nav1.8 is important in both neuropathic and inflammatory pain (Daou et al., 2016; Faber et al., 2012; Jarvis et al., 2007; Lai et al., 2002; Gold, 1999) and is acutely affected by IL-1β in DRG nociceptors (Binshtok et al., 2008). This implies that the nature of the effect and the channels affected by IL-1β depends on the duration of application. This idea is supported by the observation that 24 h hours exposure of capsaicin sensitive neurons in trigeminal ganglia to IL-1β produces an increase in TTX-S I_{Na} whereas acute exposure has no effect (Liu et al., 2006a).

4.2. Reversibility of IL-1β effects

Actions of IL-1β on different types of DRG neuron exhibit a variety of time courses and extents of reversibility. Thus, acute actions of IL-1β on nociceptor excitability and sodium currents recover within 45 min and increased excitability of medium sized DRG neurons for 5–6 days cytokine exposure recovers within 3–4 days (Binshtok et al., 2008; Stemkowski et al., 2015). IL-1β is also known to promote changes in gene expression which may reverse only extremely slowly or not at all. For example, IL-1β is known to induce both nitric oxide synthase 2 and cyclooxygenase 2 (COX-2) gene expression in DRG as well as COX-2 expression in spinal cord (Samad et al., 2001). We find that effects of IL-1β on AP amplitude and rheobase (Fig. 4a and b), that depend on TTX-S I_{Na} are reversible whereas effects on AP duration and rate of decay which depend on BK(Ca) are not (Fig. 2d and e and Fig. 4d; Table 1). This leads us to speculate that effects on BK(Ca) result from changes in gene expression either of the channels themselves or of other proteins that regulate their function. This could include alterations in intracellular Ca^{2+} buffering (Yilmaz and Gold, 2016; Yilmaz et al., 2017). In a related study, it has been shown that nerve injury reduces BK(Ca) expression in both DRG and spinal cord (Chen et al., 2009a). On the other hand, changes in TTX-S I_{Na} may reflect more rapidly reversible effects such as changes in channel phosphorylation (Viviani et al., 2003; Laedermann et al., 2015).

4.3. Use of cultured neurons

Studies were carried out on cultured neurons for several reasons. First, we wanted to expose neurons to IL-1β for periods of several days as it is known that nerve injury induced increases in IL-1β levels peak 7d after injury and remain elevated for at least an additional 7 days (Nadeau et al., 2011). As noted above, acute application of IL-1β produces different effects from longer term exposure (Liu et al., 2006b). Second, we wanted study the effect of 5-6d exposure and subsequent removal of cytokine to see if the presence of IL-1β could cause an enduring change in phenotype of IB_4^+ neurons. Such very long term

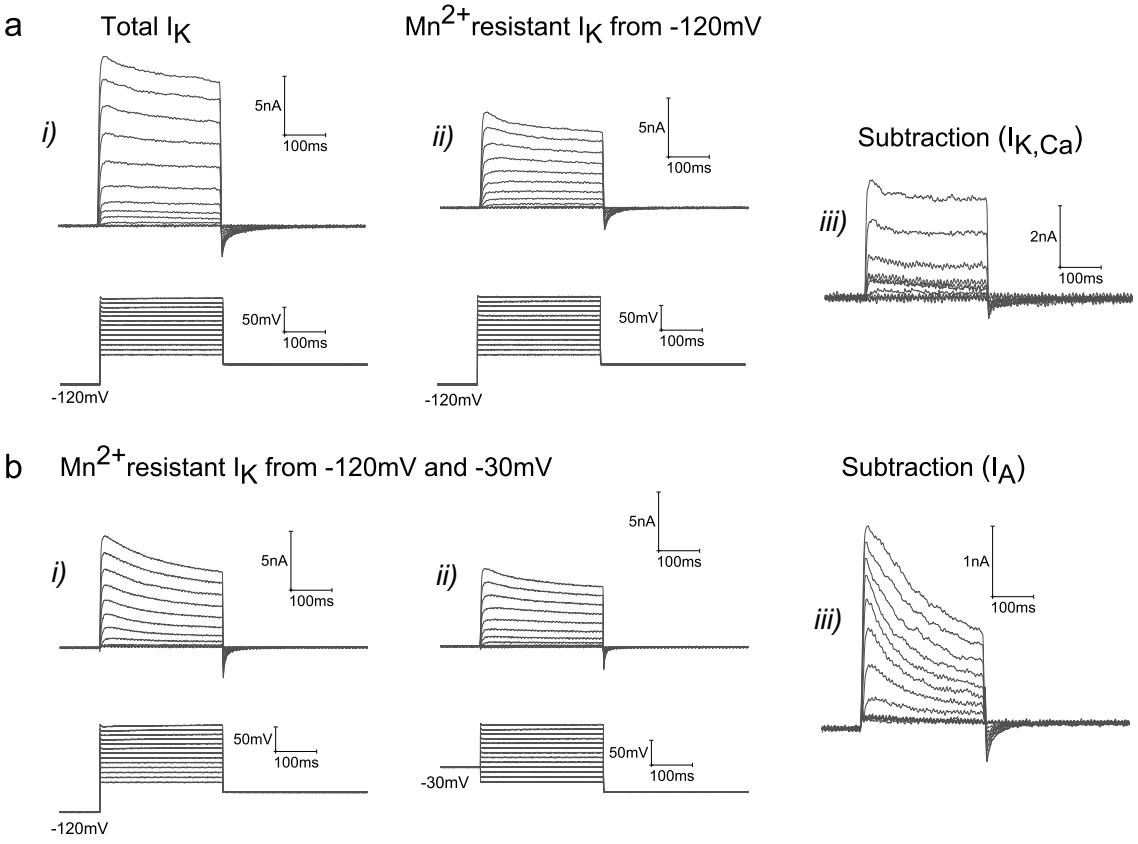

(caption on next page)

Fig. 6. Effects of IL-1β on K^+ currents in GDNF treated neurons. **a.** *i)* Typical recordings of voltage gated K^+ currents from a holding potential of -120 mV, *ii)* K^+ currents from same cell recorded in the presence of 5 mM Mn^{2+} *iii)* Subtraction of records in *ii)* from those in *i)* to reveal $I_{K,Ca}$. **b.** *i)* and *ii)*. Mn^{2+} resistant K^+ currents from another cell (recorded in presence of 5 mM Mn^{2+}) from V_h = −120 or -30 mV. *iii)* Difference in records *i)* and *ii)* reveals an inactivating current we have termed I_A. Current recorded from -30 mV is thought to represent I_{DR}. **c.**Total **c**urrent voltage plots for 18 GDNF treatred neurons and 16 GDNF treated neurons exposed to IL-1β (V_h = -120 mV). **d.** Current voltage plots for 18 GDNF treatred neurons and 18 GDNF treated neurons exposed to IL-1β and aquired in the presence of 5 mM Mn^{2+} from V_h = -30 mV (I_{DR} refer to panel **b** *ii)*). **e.** Current voltage plots for 18 GDNF treatred neurons and 18 GDNF treated neurons exposed to IL-1β and aquired in the presence of 5 mM Mn^{2+} and obtained by subtraction (I_A refer to panel **b** *iii)*). **f.** Current voltage plots for 17 GDNF treatred neurons and 16 GDNF treated neurons exposed to IL-1β and aquired by subtraction of Mn^{2+} sensitive currents from total currents ($I_{K,Ca}$ refer to panel **a** *iii)*).

experiments are only feasible in culture. Third, we wanted to study as a simple a system as possible. This is because the presence of other cell types in more intact prepartions are potential sources of cytokines and growth factors which may indirectly affect neuronal function. Lastly, we have previously reported the electrophysiological effects of IL-1β on several cell types in DRG neurons in culture (Stemkowski and Smith, 2012a; Stemkowski et al., 2015) and the present study was undertaken to further analyse the observed phenomena.

There are of course many interrelated issues with regard to the use of cell culture methodologies. These relate to the maintenance of neuronal phenotype following removal from the animal and to the fact that neurons growing in culture are axomized and no longer subject to the

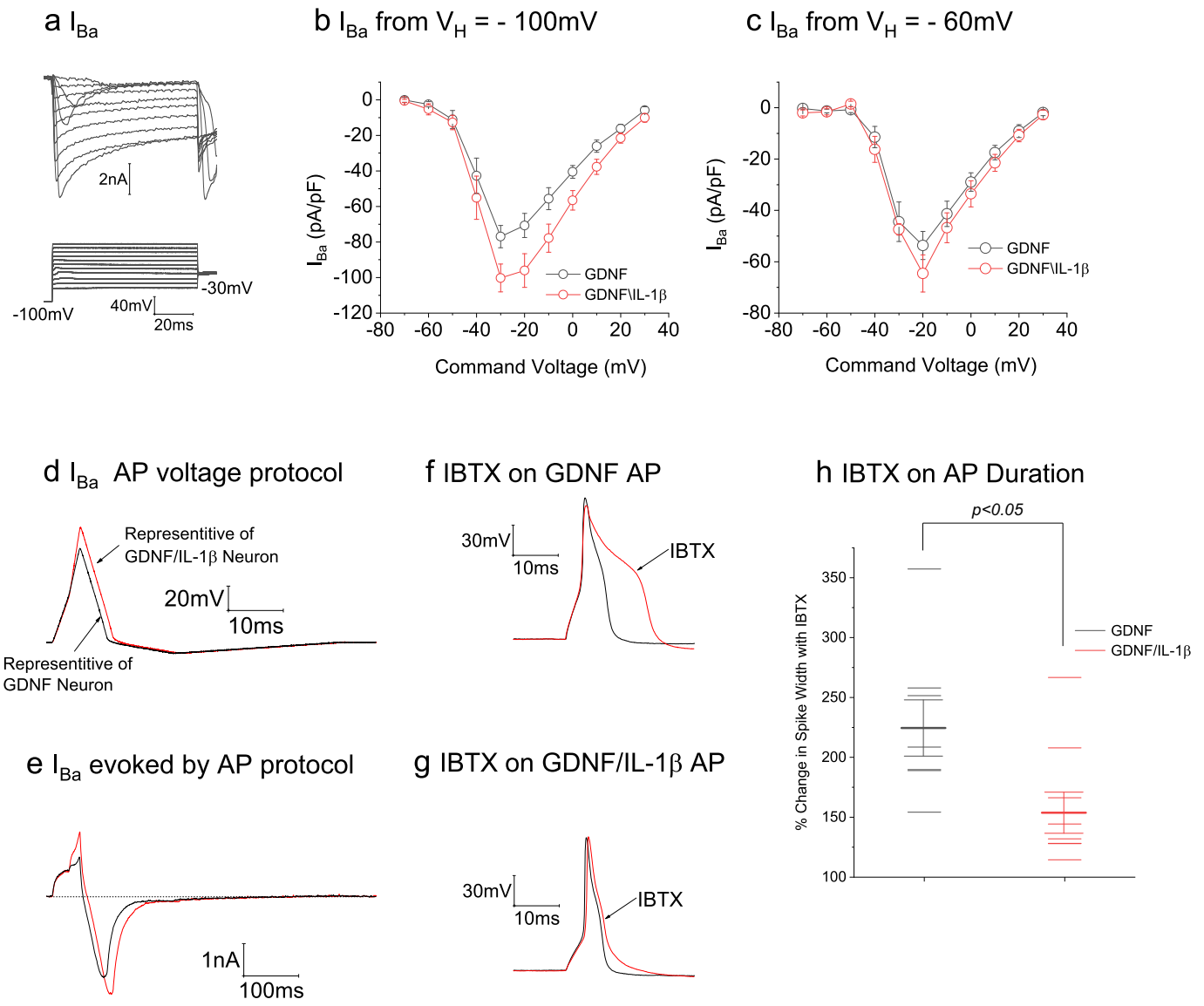

Fig. 7. Il-1β and Ca^{2+} channel currents. **a.** Typical recordings of I_{Ba} from V_h of -100 mV. **b.** Current voltage plots of I_{Ba} from V_h = -60 mV, data from 13 neurons in GDNF alone, 14 neurons in GDNF + IL-1β. Differences in currents at −30, −20 and -10 mV are not significant. **c.** Current voltage plots of I_{Ba} from V_h = -100 mV, data from 9 neurons in GDNF alone, 12 neurons in GDNF + IL-1β. Differences in currents at −30, −20 and -10 mV are not significant. **d.** Voltage protocols used to activate AP generated g_{Ba}. AP protocol representitive of a typical GDNF neuron shown in black and that typical of an IL-1β treated neuron shown in red. Protocols written in pclamp using numbers from Table 2. **e.** I_{Ba} responses evoked in a control GDNF treated neuron in response to the two voltage protocols illustrated in **d. f.** Effect of iberotoxin (IBTX, 100 nM) on AP from a control GDNF treated neuron. **g.** Effect of IBTX on AP from IL-1β treated neuron. Note attenuation of ability of IBTX to increase AP duration. **h.** Comparison of the ability of IBTX to increase AP duration in GDNF treated cells compared to similar cells that had received IL-1β. (For interpretation of the references to colour in this figure legend, the reader is referred to the web version of this article.)

action of target derived growth factors. This is especially relvant to studies of nerve injury. For example, axotomy or other types of nerve injury is known to affect expression of neuropeptides and their receptors in DRG (Rydh-Rinder et al., 1996; Xu et al., 1995; Zhang et al., 1994; Ji et al., 1994; Zhang et al., 1993; Abdulla et al., 2001). In fact, spared nerve injury has been shown to promote transient loss of IB_4 binding to DRG neurons (Hammond et al., 2004). This did not appear to happen under our culture conditions as IB_4^+ neurons were present in all experimetal situations examined. It is also possible that the percentage of IB_4^+ neurons changed with time in culture. In view of these changes it is important to emphasize that all results obtained with IL-1β exposure were measured relative to time controls. Axotomy, nerve injury or maintenance of neurons in culture has been shown to promote alterations in ion channel fuction and/or expression (Abdulla and Smith, 2001a; Abdulla and Smith, 2001b; Abdulla and Smith, 2002; Rizzo et al., 1995; Dib-Hajj et al., 1996; Cummins and Waxman, 1997) but some of these changes can be reversed by application of appropriate growth factors (Caffrey et al., 1992; Dib-Hajj et al., 1998). In view of this, studies were done on GDNF treated cultures which, as already mentioned, lends neurotophic support to IB_4^+ postive neurons and preserves the expression of TTX-R I_{Na}.

4.4. Relevance to pain mechanisms

4.4.1. Role of IL-1β

To the best of our knowledge, the effects of nerve injury on AP shape and cation currents in IB_4^+ DRG neurons have not been reported. Older literature where small DRG neurons were not subdivided into IB_4^+ and IB_4^- subpopulations showed that peripheral nerve injury increases AP duration and AP amplitude (Abdulla and Smith, 2001a) in a similar fashion to the effect of IL-1β on the IB_4^+ subpopulation (Fig. 2a and b). TTX-S I_{Na} was also increased in small DRG cells by nerve injury (Cummins and Waxman, 1997; Abdulla and Smith, 2002) and by IL-1β in the IB_4^+ subopulation (Fig. 5f). It is clear however that IL-1β modulation of ionic conductances cannot explain all of the changes produced by nerve injury. For example, nerve injury reduced delayed rectifier I_K and I_{Ca} in all types of DRG neurons (Abdulla and Smith, 2001b) but these currents were unaffected by IL-1β in IB_4^+ neurons (Fig. 6d and Fig. 7b and c). Differences likely result from actions of other inflammatory mediators such as tumor necrosis factor-α, (TNF-α), IL-6 and IL-10, all of which have implicated in neuropathic pain (Watkins and Maier, 2002) and all of which have actions on cation channels in DRG (Shen et al., 2013; Tamura et al., 2014; Leo et al., 2015; Czeschik et al., 2008;Jin and Gereau, IV, 2006; Gudes et al., 2015).

Behavioral observations strongly implicate IL-1β in the etiology of neuropathic pain. (Sommer et al., 1999; Sommer and Kress, 2004; Scholz and Woolf, 2007; Moalem and Tracey, 2006(Wolf et al., 2006; Zelenka et al., 2005)) It is also suggested that persitant activation of primary afferents is required for maintenance of central sensitization (Pitcher and Henry, 2008; Vaso et al., 2014; Sukhotinsky et al., 2004). Taken together, these findings suggest that long term exciation of DRG by IL-1β contributes to pain etiology but is it is certainly not the only inflammatory mediator involved.

4.4.2. Role of IB_4^+ neurons

As mentioned already, changes in small IB_4^+ neurons have already been implicated in the etiology of neuropathic pain (Taylor et al., 2012; Li and Zhou, 2001; Bogen et al., 2009) and in other chronic pain situations such as irritable bowel syndrome (Bautzova et al., 2018). These non-peptidergic neurons have also been implicated in a parallel pain pathway that compliments that mediated by classical peptidergic nociceptors (Braz et al., 2005). Data presented in Fig. 7d show that the change in AP shape produced by IL-1β results in increased Ca^{2+} influx. If a similar process occurs in primary afferent terminals this may result in increased neurotransmitter release and hence increased synaptic exciatation of dorsal horn neurons. This may well be the case as the observed prolongation of the AP in IB_4^+ neurons is largely due to decreases in BK(Ca) and inhibition of BK(Ca) at the spinal level with IBTX has been shown to reduce the mechanical nociceptive withdrawal threshold in control and nerve-injured rats (Chen et al., 2009a). Moreover, long term IL-1β exposure has also been reported to increase the frequency of spontaneous EPSC's in excitatory dorsal horn neurons (Gustafson-Vickers et al., 2008)

In the spinal cord, IB_4^+ neurons have been shown to synapse onto both glutamatergic vertical cells and onto GABA/glycinergic islet cells in lamina II (Peirs and Seal, 2016). Thus increased gluatamate release onto vertical cells would be expected to increase dorsal horn excitability whereas increased excitation of islet cells might be expected to have the reverse effect. It has been shown however that nerve injury causes loss of non-peptidergic terminals onto islet cells (Bailey and Ribeiro-da-Silva, 2006) and this observation is supported by the observation that nerve injury decreases synaptic drive to putative inhibitory neurons in lamina II (Balasubramanyan et al., 2006; Chen et al., 2009b).

The possibility that IL-1β selectively increases synaptic drive to excitatory neurons in the superficial dorsal horn is thus consistant with our previous observations (Gustafson-Vickers et al., 2008). In the context of the literature, our findings suggest that excitation of IB_4^+ DRG neurons by IL-1β is one of many mechanisms contributing to the central sensitization and the persistance of neuropathic pain.

Acknowledgements

Supported by Canadian Institutes of Health Research HOP 126788. PLS was supported by an Alberta Heritage Foundation for Medical Research (AHFMR) studentship and an AHFMR Dr. Lionel E. McLeod Health Research Scholarship. M-C N was supported by an Alberta Innovates Health Sciences graduate student award. We thank Ms. Twinkle Joy for technical assistance.

References

Abdulla, F.A., Smith, P.A., 1997. Nociceptin inhibits T-type Ca2+ channel current in rat sensory neurons by a G-protein-independent mechanism. J. Neurosci. 17, 8721–8728.
Abdulla, F.A., Smith, P.A., 2001a. Axotomy and Autotomy-induced changes in the excitability of rat dorsal root ganglion neurons. J. Neurophysiol. 85, 630–643.
Abdulla, F.A., Smith, P.A., 2001b. Axotomy- and Autotomy-induced changes in Ca^{2+} and K^+ channel currents of rat dorsal root ganglion neurons. J. Neurophysiol. 85, 644–658.
Abdulla, F.A., Smith, P.A., 2002. Changes in Na^+ channel currents of rat dorsal root ganglion neurons following axotomy and axotomy-induced autotomy. J. Neurophysiol. 88, 2518–2529.
Abdulla, F.A., Stebbing, M.J., Smith, P.A., 2001. Effects of substance P on excitability and ionic currents of normal and axotomized rat dorsal root ganglion neurons. Eur. J. Neurosci. 13, 545–552.
Alles, S.R.A., Smith, P.A., 2018. The Etiology and pharmacology of neuropathic pain. Pharmacol. Rev. 70, 315–347.
Baccei, M.L., Kocsis, J.D., 2000. Voltage-gated calcium currents in axotomized adult rat cutaneous afferent neurons. J. Neurophysiol. 83, 2227–2238.
Bailey, A.L., Ribeiro-da-Silva, A., 2006. Transient loss of terminals from non-peptidergic nociceptive fibers in the substantia gelatinosa of spinal cord following chronic constriction injury of the sciatic nerve. Neuroscience 138, 675–690.
Balasubramanyan, S., Stemkowski, P.L., Stebbing, M.J., Smith, P.A., 2006. Sciatic chronic constriction injury produces cell-type specific changes in the electrophysiological properties of rat *Substantia Gelatinosa* neurons. J. Neurophysiol. 96, 579–590.
Basbaum, A.I., Bautista, D.M., Scherrer, G., Julius, D., 2009. Cellular and molecular mechanisms of pain. Cell 139, 267–284.
Bautzova, T., et al., 2018. 5-oxoETE triggers nociception in constipation-predominant irritable bowel syndrome through MAS-related G protein-coupled receptor D. Sci. Signal. 11.
Binshtok, A.M., Wang, H., Zimmermann, K., Amaya, F., Vardeh, D., Shi, L., Brenner, G.J., Ji, R.R., Bean, B.P., Woolf, C.J., Samad, T.A., 2008. Nociceptors are Interleukin-1{beta} sensors. J. Neurosci. 28, 14062–14073.
Bogen, O., Joseph, E.K., Chen, X., Levine, J.D., 2008. GDNF hyperalgesia is mediated by PLCgamma, MAPK/ERK, PI3K, CDK5 and Src family kinase signaling and dependent on the IB4-binding protein versican. Eur. J. Neurosci. 28, 12–19.
Bogen, O., Dina, O.A., Gear, R.W., Levine, J.D., 2009. Dependence of monocyte chemoattractant protein 1 induced hyperalgesia on the isolectin B4-binding protein versican. Neuroscience 159, 780–786.

Braz, J.M., Nassar, M.A., Wood, J.N., Basbaum, A.I., 2005. Parallel "pain" pathways arise from subpopulations of primary afferent nociceptor. Neuron 47, 787–793.
Caffrey, J.M., Eng, D.L., Black, J.A., Waxman, S.G., Kocsis, J.D., 1992. Three types of sodium channels in adult rat dorsal root ganglion neurons. Brain Res. 592, 283–297.
Chen, S.R., Cai, Y.Q., Pan, H.L., 2009a. Plasticity and emerging role of BKCa channels in nociceptive control in neuropathic pain. J. Neurochem. 110, 352–362.
Chen, Y., Balasubramanyan, S., Lai, A.Y., Todd, K.G., Smith, P.A., 2009b. Effects of sciatic nerve Axotomy on excitatory synaptic transmission in rat Substantia Gelatinosa. J. Neurophysiol. 102, 3203–3215.
Chen, Y., Derkach, V.A., Smith, P.A., 2016. Loss of Ca(2+)-permeable AMPA receptors in synapses of tonic firing substantia gelatinosa neurons in the chronic constriction injury model of neuropathic pain. Exp. Neurol. 279, 168–177.
Choi, J.S., Dib-Hajj, S.D., Waxman, S.G., 2007. Differential slow inactivation and use-dependent inhibition of Nav1.8 channels contribute to distinct firing properties in IB4+ and IB4- DRG neurons. J. Neurophysiol. 97, 1258–1265.
Coull, J.A., Boudreau, D., Bachand, K., Prescott, S.A., Nault, F., Sik, A., De Koninck, P., de Koninck, Y., 2003. Trans-synaptic shift in anion gradient in spinal lamina I neurons as a mechanism of neuropathic pain. Nature 424, 938–942.
Cummins, T.R., Waxman, S.G., 1997. Downregulation of TTX-resistant sodium currents and Upregulation of a rapidly TTX-Senstive sodium current in small spinal sensory neurons after nerve injury. J. Neurosci. 17, 3503–3514.
Cummins, T.R., Black, J.A., Dib-Hajj, S.D., Waxman, S.G., 2000. Glial-derived neurotrophic factor upregulates expression of functional SNS and NaN sodium channels and their currents in axotomized dorsal root ganglion neurons. J. Neurosci. 20, 8754–8761.
Czeschik, J.C., Hagenacker, T., Schafers, M., Busselberg, D., 2008. TNF-alpha differentially modulates ion channels of nociceptive neurons. Neurosci. Lett. 434, 293–298.
Daou, I., Beaudry, H., Ase, A.R., Wieskopf, J.S., Ribeiro-da-Silva, A., Mogil, J.S., Seguela, P., 2016. Optogenetic silencing of Nav1.8-positive afferents alleviates inflammatory and neuropathic pain. eNeuro 3.
Decosterd, I., Woolf, C.J., 2000. Spared nerve injury: an animal model of persistent peripheral neuropathic pain. Pain 87, 149–158.
Dib-Hajj, S., Black, J.A., Felts, P., Waxman, S.G., 1996. Down-regulation of transcripts for Na channel alpha-SNS in spinal sensory neurons following axotomy. Proc. Natl. Acad. Sci. U. S. A. 93, 14950–14954.
Dib-Hajj, S.D., Black, J.A., Cummins, T.R., Kenney, A.M., Kocsis, J.D., Waxman, S.G., 1998. Rescue of alpha-SNS sodium channel expression in small dorsal root ganglion neurons after axotomy by nerve growth factor in vivo. J. Neurophysiol. 79, 2668–2676.
Djouhri, L., Koutsikou, S., Fang, X., McMullan, S., Lawson, S.N., 2006. Spontaneous pain, both neuropathic and inflammatory, is related to frequency of spontaneous firing in intact C-fiber nociceptors. J. Neurosci. 26, 1281–1292.
Faber, C.G., Lauria, G., Merkies, I.S., Cheng, X., Han, C., Ahn, H.S., Persson, A.K., Hoeijmakers, J.G., Gerrits, M.M., Pierro, T., Lombardi, R., Kapetis, D., Dib-Hajj, S.D., Waxman, S.G., 2012. Gain-of-function Nav1.8 mutations in painful neuropathy. Proc. Natl. Acad. Sci. U. S. A. 109, 19444–19449.
Fang, X., Djouhri, L., McMullan, S., Berry, C., Waxman, S.G., Okuse, K., Lawson, S.N., 2006. Intense isolectin-B4 binding in rat dorsal root ganglion neurons distinguishes C-fiber nociceptors with broad action potentials and high Nav1.9 expression. J. Neurosci. 26, 7281–7292.
Ferrari, L.F., Bogen, O., Levine, J.D., 2010. Nociceptor subpopulations involved in hyperalgesic priming. Neuroscience 165, 896–901.
Ferreira, S.H., Lorenzetti, B.B., Bristow, A.F., Poole, S., 1988. Interleukin-1 beta as a potent hyperalgesic agent antagonized by a tripeptide analogue. Nature 334, 698–700.
Fjell, J., Cummins, T.R., Dib-Hajj, S.D., Fried, K., Black, J.A., Waxman, S.G., 1999. Differential role of GDNF and NGF in the maintenance of two TTX- resistant sodium channels in adult DRG neurons. Brain Res. Mol. Brain Res. 67, 267–282.
Gold, M.S., 1999. Tetrodotoxin-resistant Na+ currents and inflammatory hyperalgesia. Proc. Natl. Acad. Sci. U. S. A. 96, 7645–7649.
Gold, M.S., Shuster, M.J., Levine, J.D., 1996. Characterization of six voltage-gated K+ currents in adult rat sensory neurons. J. Neurophysiol. 75, 2629–2646.
Golden, J.P., Hoshi, M., Nassar, M.A., Enomoto, H., Wood, J.N., Milbrandt, J., Gereau, R.W., Johnson Jr., E.M., Jain, S., 2010. RET signaling is required for survival and normal function of nonpeptidergic nociceptors. J. Neurosci. 30, 3983–3994.
Grace, P.M., Hutchinson, M.R., Maier, S.F., Watkins, L.R., 2014. Pathological pain and the neuroimmune interface. Nat. Rev. Immunol. 14, 217–231.
Gudes, S., Barkai, O., Caspi, Y., Katz, B., Lev, S., Binshtok, A.M., 2015. The role of slow and persistent TTX-resistant sodium currents in acute tumor necrosis factor-alpha-mediated increase in nociceptors excitability. J. Neurophysiol. 113, 601–619.
Gustafson-Vickers, S.L., Lu, V.B., Lai, A.Y., Todd, K.G., Ballanyi, K., Smith, P.A., 2008. Long-term actions of interleukin-1beta on delay and tonic firing neurons in rat superficial dorsal horn and their relevance to central sensitization. Mol. Pain 4, 63.
Hammond, D.L., Ackerman, L., Holdsworth, R., Elzey, B., 2004. Effects of spinal nerve ligation on immunohistochemically identified neurons in the L4 and L5 dorsal root ganglia of the rat. J. Comp. Neurol. 475, 575–589.
Harper, A.A., Lawson, S.N., 1985. Conduction velocity is related to morphological cell type in rat dorsal root ganglion neurones. J. Physiol. Lond. 359, 31–46.
Hunt, S.P., Mantyh, P.W., 2001. The molecular dynamics of pain control. Nat. Rev. Neurosci. 2, 83–91.
Jarvis, M.F., et al., 2007. A-803467, a potent and selective Nav1.8 sodium channel blocker, attenuates neuropathic and inflammatory pain in the rat. Proc. Natl. Acad. Sci. U. S. A. 104, 8520–8525.
Ji, R.R., Zhang, X., Wiesenfeld-Hallin, Z., Hokfelt, T., 1994. Expression of neuropeptide Y and neuropeptide Y (Y1) receptor mRNA in rat spinal cord and dorsal root ganglia following peripheral tissue inflammation. J. Neurosci. 14, 6423–6434.
Jin, X., Gereau IV, R.W., 2006. Acute p38-mediated modulation of Tetrodotoxin-resistant sodium channels in mouse sensory neurons by tumor necrosis factor-{alpha}. J. Neurosci. 26, 246–255.
Kim, K.J., Yoon, Y.W., Chung, J.M., 1997. Comparison of three rodent models of neuropathic pain. Exp. Brain Res. 113, 200–206.
Koplovitch, P., Devor, M., 2018. Dilute lidocaine suppresses ectopic neuropathic discharge in dorsal root ganglia without blocking axonal propagation: a new approach to selective pain control. Pain 159, 1244–1256.
Laedermann, C.J., Abriel, H., Decosterd, I., 2015. Post-translational modifications of voltage-gated sodium channels in chronic pain syndromes. Front. Pharmacol. 6, 263.
Lai, J., Gold, M.S., Kim, C.S., Biana, D., Ossipov, M.H., Hunterc, J.C., Porreca, F., 2002. Inhibition of neuropathic pain by decreased expression of the tetrodotoxin-resistant sodium channel, NaV1.8. Pain 95, 143–152.
Leo, M., Argalski, S., Schafers, M., Hagenacker, T., 2015. Modulation of voltage-gated sodium channels by activation of tumor necrosis factor Receptor-1 and Receptor-2 in small DRG neurons of rats. Mediat. Inflamm. 2015, 124942.
Li, L., Zhou, X.F., 2001. Pericellular Griffonia simplicifolia I isolectin B4-binding ring structures in the dorsal root ganglia following peripheral nerve injury in rats. J. Comp. Neurol. 439, 259–274.
Liu, L., Yang, T.M., Liedtke, W., Simon, S.A., 2006a. Chronic IL-1beta Signaling potentiates voltage-dependent sodium currents in trigeminal nociceptive neurons. J. Neurophysiol. 95, 1478–1490.
Liu, L., Yang, T.M., Liedtke, W., Simon, S.A., 2006b. Chronic IL-1beta Signaling potentiates voltage-dependent sodium currents in trigeminal nociceptive neurons. J. Neurophysiol. 95, 1478–1490.
Lu, K.T., Wang, Y.W., Wo, Y.Y., Yang, Y.L., 2005. Extracellular signal-regulated kinase-mediated IL-1-induced cortical neuron damage during traumatic brain injury. Neurosci. Lett. 386, 40–45.
MacGillivray, M.K., Cruz, T.F., McCulloch, C.A., 2000. The recruitment of the interleukin-1 (IL-1) receptor-associated kinase (IRAK) into focal adhesion complexes is required for IL-1beta -induced ERK activation. J. Biol. Chem. 275, 23509–23515.
Moalem, G., Tracey, D.J., 2006. Immune and inflammatory mechanisms in neuropathic pain. Brain Res. Rev. 51, 240–264.
Molliver, D.C., Radeke, M.J., Feinstein, S.C., Snider, W.D., 1995. Presence or absence of TrkA protein distinguishes subsets of small sensory neurons with unique cytochemical characteristics and dorsal horn projections. J. Comp. Neurol. 361, 404–416.
Molliver, D.C., Wright, D.E., Leitner, M.L., Parsadanian, A.S., Doster, K., Wen, D., Yan, Q., Snider, W.D., 1997. IB4-binding DRG neurons switch from NGF to GDNF dependence in early postnatal life. Neuron 19, 849–861.
Nadeau, S., Filali, M., Zhang, J., Kerr, B.J., Rivest, S., Soulet, D., Iwakura, Y., de Rivero Vaccari, J.P., Keane, R.W., Lacroix, S., 2011. Functional recovery after peripheral nerve injury is dependent on the pro-inflammatory cytokines IL-1beta and TNF: implications for neuropathic pain. J. Neurosci. 31, 12533–12542.
Peirs, C., Seal, R.P., 2016. Neural circuits for pain: recent advances and current views. Science 354, 578–584.
Pitcher, G.M., Henry, J.L., 2008. Governing role of primary afferent drive in increased excitation of spinal nociceptive neurons in a model of sciatic neuropathy. Exp. Neurol. 214, 219–228.
Rizzo, M.A., Kocsis, J.D., Waxman, S.G., 1995. Selective loss of slow and enhancement of fast Na^+ currents in cutaneous afferent dorsal root ganglion neurons following axotomy. Neurobiol. Dis. 2, 87–96.
Robinson, D.R., McNaughton, P.A., Evans, M.L., Hicks, G.A., 2004. Characterization of the primary spinal afferent innervation of the mouse colon using retrograde labelling. Neurogastroenterol. Motil. 16, 113–124.
Rydh-Rinder, M., Holmberg, K., Elfvin, L.G., Wiesenfeld-Hallin, Z., Hokfelt, T., 1996. Effects of peripheral axotomy on neuropeptides and nitric oxide synthase in dorsal root ganglia and spinal cord of the Guinea pig: an immunohistochemical study. Brain Res. 707, 180–188.
Samad, T.A., Moore, K.A., Sapirstein, A., Billet, S., Allchorne, A., Poole, S., Bonventre, J.V., Woolf, C.J., 2001. Interleukin-1beta-mediated induction of cox-2 in the CNS contributes to inflammatory pain hypersensitivity. Nature 410, 471–475.
Sandkuhler, J., 2009. Models and mechanisms of hyperalgesia and allodynia. Physiol. Rev. 89, 707–758.
Scholz, J., Woolf, C.J., 2007. The neuropathic pain triad: neurons, immune cells and glia. Nat. Neurosci. 10, 1361–1368.
Shen, K.F., Zhu, H.Q., Wei, X.H., Wang, J., Li, Y.Y., Pang, R.P., Liu, X.G., 2013. Interleukin-10 down-regulates voltage gated sodium channels in rat dorsal root ganglion neurons. Exp. Neurol. 247, 466–475.
Silverman, J.D., Kruger, L., 1990. Selective neuronal glycoconjugate expression in sensory and autonomic ganglia: relation of lectin reactivity to peptide and enzyme markers. J. Neurocytol. 19, 789–801.
Snape, A., Pittaway, J.F., Baker, M.D., 2010. Excitability parameters and sensitivity to anemone toxin ATX-II in rat small diameter primary sensory neurones discriminated by Griffonia simplicifolia isolectin IB4. J. Physiol. (Lond) 588, 125–137.
Sommer, C., Kress, M., 2004. Recent findings on how proinflammatory cytokines cause pain: peripheral mechanisms in inflammatory and neuropathic hyperalgesia. Neurosci. Lett. 361, 184–187.
Sommer, C., Petrausch, S., Lindenlaub, T., Toyka, K.V., 1999. Neutralizing antibodies to interleukin 1-receptor reduce pain associated behavior in mice with experimental neuropathy. Neurosci. Lett. 270, 25–28.
Stemkowski, P.L., Smith, P.A., 2012a. Long-term IL-1beta exposure causes subpopulation-dependent alterations in rat dorsal root ganglion neuron excitability. J. Neurophysiol. 107, 1586–1597.
Stemkowski, P.L., Smith, P.A., 2012b. Sensory neurons, ion channels, inflammation and the onset of neuropathic pain. Can. J. Neurol. Sci. 39, 416–435.
Stemkowski, P.L., Smith, P.A., 2013. An overview of animal models of neuropathic pain.

In: Toth, C., Moulin, D.E. (Eds.), Neuropathic Pain, Causes, Management and Understanding. Cambridge University Press, pp. 33–50.
Stemkowski, P.L., Noh, M.C., Chen, Y., Smith, P.A., 2015. Increased excitability of medium-sized dorsal root ganglion neurons by prolonged interleukin-1beta exposure is K(+) channel dependent and reversible. J. Physiol. 593, 3739–3755.
Stucky, C.L., Lewin, G.R., 1999. Isolectin B(4)-positive and -negative nociceptors are functionally distinct. J. Neurosci. 19, 6497–6505.
Sukhotinsky, I., Ben Dor, E., Raber, P., Devor, M., 2004. Key role of the dorsal root ganglion in neuropathic tactile hypersensibility. Eur. J. Pain 8, 135–143.
Tamura, R., Nemoto, T., Maruta, T., Onizuka, S., Yanagita, T., Wada, A., Murakami, M., Tsuneyoshi, I., 2014. Up-regulation of NaV1.7 sodium channels expression by tumor necrosis factor-alpha in cultured bovine adrenal chromaffin cells and rat dorsal root ganglion neurons. Anesth. Analg. 118, 318–324.
Taylor, A.M., Osikowicz, M., Ribeiro-da-Silva, A., 2012. Consequences of the ablation of nonpeptidergic afferents in an animal model of trigeminal neuropathic pain. Pain 153, 1311–1319.
Vaso, A., Adahan, H.M., Gjika, A., Zahaj, S., Zhurda, T., Vyshka, G., Devor, M., 2014. Peripheral nervous system origin of phantom limb pain. Pain 155, 1384–1391.
Viviani, B., Bartesaghi, S., Gardoni, F., Vezzani, A., Behrens, M.M., Bartfai, T., Binaglia, M., Corsini, E., Di Luca, M., Galli, C.L., Marinovich, M., 2003. Interleukin-1beta enhances NMDA receptor-mediated intracellular calcium increase through activation of the Src family of kinases. J. Neurosci. 23, 8692–8700.
Wall, P.D., Devor, M., 1983. Sensory afferent impulses result from dorsal root ganglia as well as from the periphery in normal and nerve-injured rats. Pain 17, 321–339.
Watkins, L.R., Maier, S.F., 2002. Beyond neurons: evidence that immune and glial cells contribute to pathological pain states. Physiol. Rev. 82, 981–1011.
Waxman, S.G., Zamponi, G.W., 2014. Regulating excitability of peripheral afferents: emerging ion channel targets. Nat. Neurosci. 17, 153–163.
Wolf, G., Gabay, E., Tal, M., Yirmiya, R., Shavit, Y., 2006. Genetic impairment of interleukin-1 signaling attenuates neuropathic pain, autotomy, and spontaneous ectopic neuronal activity, following nerve injury in mice. Pain 120, 315–324.
Woolf, C.J., 1983. Evidence for a central component of post-injury pain hypersensitivity. Nature 306, 686–688.
Xu, X.J., Andell, S., Zhang, X., Wiesenfeld-Hallin, Z., Langel, U., Bedecs, K., Hokfelt, T., Bartfai, T., 1995. Peripheral axotomy increases the expression of galanin message-associated peptide (GMAP) in dorsal root ganglion cells and alters the effects of intrathecal GMAP on the flexor reflex in the rat. Neuropeptides 28, 299–307.
Yilmaz, E., Gold, M.S., 2016. Paclitaxel-induced increase in NCX activity in subpopulations of nociceptive afferents: a protective mechanism against chemotherapy-induced peripheral neuropathy? Cell Calcium 60, 25–31.
Yilmaz, E., Watkins, S.C., Gold, M.S., 2017. Paclitaxel-induced increase in mitochondrial volume mediates dysregulation of intracellular Ca2+ in putative nociceptive glabrous skin neurons from the rat. Cell Calcium 62, 16–28.
Yunoki, T., Takimoto, K., Kita, K., Funahashi, Y., Takahashi, R., Matsuyoshi, H., Naito, S., Yoshimura, N., 2014. Differential contribution of Kv4-containing channels to A-type, voltage-gated potassium currents in somatic and visceral dorsal root ganglion neurons. J. Neurophysiol. 112, 2492–2504.
Zelenka, M., Schafers, M., Sommer, C., 2005. Intraneural injection of interleukin-1beta and tumor necrosis factor-alpha into rat sciatic nerve at physiological doses induces signs of neuropathic pain. Pain 116, 257–263.
Zhang, X., Ju, G., Elde, R., Hokfelt, T., 1993. Effect of peripheral nerve cut on neuropeptides in dorsal root ganglia and the spinal cord of monkey with special reference to galanin. J. Neurocytol. 22, 342–381.
Zhang, X., Wiesenfeld-Hallin, Z., Hokfelt, T., 1994. Effect of peripheral axotomy on expression of neuropeptide Y receptor mRNA in rat lumbar dorsal root ganglia. Eur. J. Neurosci. 6, 43–57.
Zwick, M., Davis, B.M., Woodbury, C.J., Burkett, J.N., Koerber, H.R., Simpson, J.F., Albers, K.M., 2002. Glial cell line-derived neurotrophic factor is a survival factor for isolectin B4-positive, but not vanilloid receptor 1-positive, neurons in the mouse. J. Neurosci. 22, 4057–4065.